Bull. Astr. Soc. India (2004) **32**, 169–183

Occurrence of thermal instability in molecular clouds

Mohsen Nejad-Asghar*
Jamshid Ghanbari†
Department of Physics, School of Sciences,Ferdowsi University of Mashhad, Mashhad, Iran

Received 18 June 2004; accepted 10 August 2004

Abstract. Linear perturbation is used on the complete MHD equations of the magnetic molecular clouds. We carry out a comparison of characteristic time-scales, and find conditions which linear thermal instability causes to form the small-scale condensations in the local expanding/contracting medium of a molecular cloud. We consider the ambipolar diffusion, or ion-neutral friction on the perturbed states. In this way, we obtain a non-dimensional characteristic equation that reduces to the prior characteristic equation in the non-gravitating stationary background. By manipulation of this characteristic equation, we conclude that there are, not only oblate formation regions, but also prolate condensation forming solutions, according to expansion or contraction of the background. Some typical data that correspond to the real observed magnetic molecular clouds is presented.

Keywords : ISM: clouds, ISM: molecules, ISM: structure, instabilities, magnetohydrodynamics: MHD, star: formation

1. Introduction

Evidence of small-scale condensations (clumps) in the magnetic molecular clouds has been accumulating over the past decades through radio and optical/ultraviolet observations. Direct imaging of ^{12}CO in nearby clouds reveals substructures on all scales down to lengths of $\sim 0.01pc$ and masses of $\sim 0.01M_{\odot}$ (Peng et al. 1998, Sakamoto & Sunada 2003). Studies of the time variability of absorption lines indicates the presence of small-scale condensations in the dense gas on scales down to lengths of $\sim 5\times10^{-5}pc$ ($\sim 10AU$)

*School of Physics, Damghan University of Sciences, Damghan, Iran, e-mail:nasghar@dubs.ac.ir
†e-mail:ghanbari@ferdowsi.um.ac.ir

and masses of $\sim 5 \times 10^{-9} M_\odot$ (Moore & Marscher 1995, Liszt & Lucas 2000, Rollinde et al. 2003).

As a general rule, neither sub-parsec clumps nor AU-scale condensations are spherical (Ryden 1996). Jones & Basu (2002) have recently deciphered intrinsic three-dimensional shape distributions of molecular clouds, cloud cores, Bok globules, and small-scale condensations. They use recently compiled catalogues of observed axis ratios for these objects mapped in carbon monoxide, in ammonia, through optical selection, or in continuum dust emission. They find out that molecular clouds mapped in ^{12}CO are intrinsically triaxial but more nearly prolate than oblate, while the smaller cloud cores, Bok globules, and small-scale condensations are also intrinsically triaxial but more nearly oblate than prolate.

Small-scale condensations appear to be immediate precursors of large-scale clumps (dense cores with significant Jeans mass) via merging and collisions; they constitute the initial conditions for star formation. Therefore, understanding of the origin and merging of these small-scale condensations is of fundamental importance for a consistent theory of star formation and galactic evolution.

The origin and shape of these small-scale condensations is a disputable issue. Non-isotropic heating and fragmentation via gravitational collapse is an important reason for oblate/prolate large-scale clumps with significant Jeans mass (e.g. Nelson & Langer 1997, Indebetouw & Zweibel 2000, Hartmann 2002). The above scenario is not correct for small-scale condensations, because they have low gas density and small sizes, thus, their masses are significantly smaller than their corresponding Jeans mass. According to this feature, the only remaining responsible agents may be *turbulence* and/or *thermal instability*.

Gammie et al. (2003) have recently studied the effect of turbulence in three dimensional analogs of clumps using a set of self consistent, time-dependent, numerical models of molecular clouds. The models follow the decay of initially supersonic turbulence in an isothermal, self-gravitating, magnetized fluid. They have concluded that nearly 90% of the clumps are formed in prolate and 10% of them are oblate.

In molecular clouds, the dispersion velocity inferred from molecular line width is often larger than the gas sound speed inferred from transition temperatures (Solomon et al 1987). Magnetohydrodynamic turbulence may be responsible for the stirring of these clouds (Arons & Max 1975). Because of these turbulent motions, molecular clouds must have transient structure, and are probably dispersed after not much more than $\sim 10^7 yr$ (Larson 1981). Since cooling time-scale of molecular clouds is approximately $\sim 10^3 - 10^4 yr$ (Gilden 1984), thermal instability must be a coordinated trigger mechanism to form condensations. Turbulence, in the second stage, can deform these small-scale condensations in shape, and orient them relative to the background magnetic field.

Observations and theoretical studies establish that magnetic fields play an important role in shaping the structure and dynamics of molecular clouds and their substructures (e.g. Basu 2000, Fiege & Pudritz 2000, Hennebelle 2003). The relative alignment of the projected magnetic field with the projected minor axis of the condensations is an important diagnostic.

In conformity with the above explanation, Nejad-Asghar & Ghanbari (2003 hereafter NG) investigated the effect of ambipolar diffusion on the thermal instability and formation of small-scale condensations in a homogeneous magnetic molecular cloud. They concluded that there are solutions where the thermal instability allows compression along the magnetic field but not perpendicular to it. NG inferred that this aspect might be evidence in formation of the observed oblate small-scale condensations in magnetic molecular clouds.

In this paper we want to test and develop the work of NG, by including self-gravity and local contracting/expanding background. We present the basic equations, background evolution, and the linearized equations in section 2. Section 3 compares the relative time-scales and some numerical data of the molecular clouds which, culminates in different shapes of condensation. A summary of the results and some future prospects are discussed in section 4.

2. The equations of the problem

The basic equations, including self-gravity and ambipolar diffusion, are given first in general (§2.1). They are specialized for the local homogeneous contracting/expanding molecular cloud (§2.2), and for small perturbations to that medium (§2.3).

2.1 Equations

A molecular cloud gas includes neutral atoms and molecules, atomic and molecular ions, and electrons, which are the primary current carriers. Since significant charge separation cannot be sustained on the astrophysical time-scales, we find that the electrons and ions move together.

In principle, the ion velocity, $\boldsymbol{v}_i$, and the neutral velocity, $\boldsymbol{v}_n$, should be determined by solving separate fluid equations for these species, including their coupling by collision processes (Draine 1986). But, in the time-scale of cooling considered here, ($10^3 - 10^4 yr$, Gilden 1984), the ion and neutral fluids are well coupled together, and we can use the basic equations as follows (Shu 1992)

$$\frac{d\rho}{dt} + \rho \nabla \cdot \boldsymbol{v} = 0 \tag{1}$$

$$\rho\frac{d\boldsymbol{v}}{dt}+\nabla p+\nabla(\frac{B^2}{8\pi})-(\mathbf{B}\cdot\nabla)\frac{\mathbf{B}}{4\pi}+\rho\nabla\psi=0 \tag{2}$$

$$\frac{1}{\gamma-1}\frac{dp}{dt}-\frac{\gamma}{\gamma-1}\frac{p}{\rho}\frac{d\rho}{dt}+\rho\Omega-\nabla\cdot(K\nabla T)=0 \tag{3}$$

$$\frac{d\mathbf{B}}{dt}+\mathbf{B}(\nabla\cdot\boldsymbol{v})-(\mathbf{B}\cdot\nabla)\boldsymbol{v}=\nabla\times(\boldsymbol{v}_d\times\mathbf{B}) \tag{4}$$

$$\nabla^2\psi=4\pi G\rho \tag{5}$$

$$p-\frac{R}{\mu}\rho T=0 \tag{6}$$

where all symbols have their usual meaning and

$$\boldsymbol{v}_d\equiv\frac{1}{4\pi\eta\epsilon\rho^{1+\nu}}[(\nabla\times\mathbf{B})\times\mathbf{B}] \tag{7}$$

is the drift velocity of ions. $\eta=\frac{<v_{in}\sigma_{in}>}{m_i+m_n}$ is the collision drag where v_{in} is the ion-neutral relative velocity with impinging cross section σ_{in}. The averaged collision rate $< v_{in}\sigma_{in} >$ is calculated by using Langevin's approximation for the polarization potential, $V_p=-\alpha_n e^2/2r^4$, where α_n is the mean dipole polarizability of neutrals, and e is the electronic charge. One finds that $< v_{in}\sigma_{in} >= 2.21\pi(\alpha_n e^2/m_i)^{1/2}$ where $\alpha_n = 8.08\times10^{-5}cm^3$ for hydrogen molecules (see McDaniel & Mason 1973). Thus, the collision drag is $\eta = 2.46\times10^{14}cm^3.gr^{-1}.s^{-1}$. We use the relation $\rho_i=\epsilon\rho_n^\nu$ ($\epsilon=1.83\times10^{-17}cm^{-3/2}.gr^{1/2}$, $\nu=1/2$) between ion and neutral densities in molecular clouds (Umebayasi & Nakano 1980), and we approximate $\rho=\rho_n+\rho_i\approx\rho_n$.

The net cooling function ($erg.gr^{-1}.sec^{-1}$) is

$$\Omega(\rho,T)=\Lambda(\rho,T)-\Gamma_{tot} \tag{8}$$

where Γ_{tot} is the total heating rate and $\Lambda(\rho,T)$ is the cooling rate which can be written as (Goldsmith & Langer 1978, Neufeld et al. 1995)

$$\Lambda(\rho,T)=\Lambda_0\rho^\delta T^\beta \tag{9}$$

where Λ_0, δ, and β are constants. The range of β is 1.4 to 2.9. The constant δ is greater than zero for the optically thin case and less than zero for the optically thick case (see Fig. 1). Models of the molecular clouds identify several different heating mechanisms. In this paper, we consider the heating rates of cosmic rays, H_2 formation, H_2 dissociation, grain photoelectrons, and collisions with warm dust as a constant Γ_0 (Glassgold & Langer 1974, Goldsmith & Langer 1978). The heating of the gas by magnetic ion-neutral slip is

$$\Gamma_{AD}=\frac{\boldsymbol{f}_d\cdot\boldsymbol{v}_d}{\rho_n} \tag{10}$$

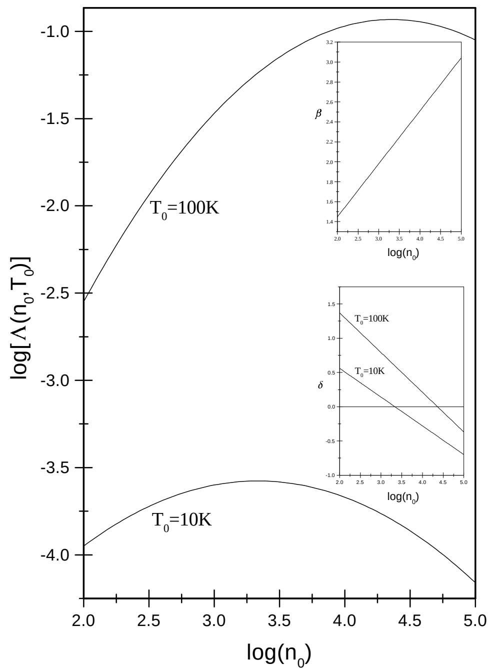

Figure 1. Logarithm of the cooling rate, $\Lambda(n_0, T_0) = \Lambda_0 n_0^\delta T_0^\beta$, versus number density in molecular clouds, $n_0(cm^{-3})$, according to Goldsmith & Langer (1978). The best fit results for the values of δ and β are shown in this figure.

where $\boldsymbol{f}_d = \eta\epsilon\rho^{1+\nu}$ is the drag force (per unit volume). If κB_0 changes on a typical scale of λ, the ambipolar diffusion heating rate, is given by

$$\Gamma_{AD} = \Gamma_0' \rho^{-(2+\nu)}; \quad \Gamma_0' \equiv \frac{(\kappa B_0)^4}{16\pi^2 \eta\epsilon\lambda^2}. \tag{11}$$

The gravitational heating rate is found by setting the rate of contraction/expansion work per particle, $pd(n^{-1})/dt$, equal to the rate of change of gravitational energy per particle, $[d(PE_{tot})/dt]/(nV)$, where PE_{tot} is the total gravitational potential energy of the volume V. For a uniform sphere of radius λ we find, approximately,

$$\Gamma_{grav} = \Gamma_0'' \rho^{3/2}, \quad \Gamma_0'' \equiv \frac{(4\pi G)^{3/2}}{5\sqrt{3}} [-\dot{a}(\tau)]\lambda^2 \tag{12}$$

where $\dot{a}(\tau)$ is the contraction/expansion parameter rate (see §2.2).

2.2 Background Evolution

As a basis for the small-perturbation analysis, we assume a local homogeneous background which is expanding/contracting uniformly, so that the unperturbed quantities only depend on time. The background quantities will be denoted with the subscript 0. The contraction/expansion is given by

$$\boldsymbol{r} = a_{(t)}\boldsymbol{x} \tag{13}$$

where $\boldsymbol{r}$ is the Eulerian coordinate, $\boldsymbol{x}$ is the Lagrangian coordinate and $a_{(t)}$ is the expansion/contraction parameter. Using equation (13), the unperturbed velocity field is given by

$$\boldsymbol{v}_0 = \frac{da/dt}{a}\boldsymbol{r}. \tag{14}$$

For background evolution, the basic equations (1)-(6) reduce to

$$\rho_{0(t)} = \rho_{0(t=0)} a_{(t)}^{-3}, \quad p_{0(t)} = p_{0(t=0)} a_{(t)}^{-3\gamma} \tag{15}$$

$$T_{0(t)} = T_{0(t=0)} a_{(t)}^{-3(\gamma-1)}, \quad \mathbf{B}_{0(t)} = \mathbf{B}_{0(t=0)} a_{(t)}^{-2} \tag{16}$$

where $a_{(t)}$ follow the differential equation

$$a_{(\tau)}\dot{a}_{(\tau)} = -1 \tag{17}$$

where the $\dot{a}$ indicates its derivative with respect to a defined non-dimensional variable $\tau \equiv [\frac{4}{3}\pi G\rho_0(t=0)]^{1/2}t$. The initial conditions for $a_{(\tau)}$, appropriate for molecular clouds, are

$$a_{(\tau=0)} = 1, \quad \dot{a}_{(\tau=0)} = \pm 0.01 - \pm 1.0 \tag{18}$$

where the plus sign corresponds to initial expansion, and the minus corresponds to initial contraction. A suitable function in the range of $0 \leq \tau \leq 0.1$, is

$$a_{(\tau)} = 1 + \dot{a}_{(\tau=0)}\tau - 0.5\tau^2. \tag{19}$$

2.3 Linearized Equations

Density fluctuation ratios in the molecular substructures is in the order of ~ 10 (Falgarone et al. 1992, Pan et al. 2001). Therefore, the linear regime of the thermal instability might lead to some significant results for small-scale condensation formation.

To obtain a linearized system of equations, we split each variable into unperturbed and perturbed components, indicating the latter with a subscript 1. Eulerian divergence operator is applied to the equations (1)-(6), then all equations are rewritten in terms of the Lagrangian coordinate $\boldsymbol{x}$. The resulting linear system has coefficients which depend on t but not on $\boldsymbol{x}$. We then carry out a spatial Fourier analysis, with Fourier components proportional to $exp(i\boldsymbol{k}\cdot\boldsymbol{x})$, so that $\boldsymbol{k}$ is the Lagrangian wave vector.

Simplifying the resulting linear system by repeated use of the background equation (15) and (16), we obtain

$$\frac{d}{dt}(\frac{\rho_1}{\rho_0})+i\tilde{\boldsymbol{k}}\cdot\boldsymbol{v}_1=0 \tag{20}$$

$$\frac{d\boldsymbol{v}_1}{dt}+\frac{da/at}{a}\boldsymbol{v}_1+i\frac{c_s}{\gamma\tau_s}\frac{\tilde{\boldsymbol{k}}}{\tilde{k}}(\frac{p_1}{p_0})+i\frac{\mathbf{B}_0\cdot\mathbf{B}_1}{4\pi\rho_0}\tilde{\boldsymbol{k}}-i\frac{\tilde{\boldsymbol{k}}\cdot\mathbf{B}_0}{4\pi\rho_0}\mathbf{B}_1-i\frac{\tilde{\boldsymbol{k}}}{\tilde{k}^2\tau_g^2}(\frac{\rho_1}{\rho_0})=0 \tag{21}$$

$$\frac{d}{dt}(\frac{p_1}{p_0})+i\gamma\tilde{\boldsymbol{k}}\cdot\boldsymbol{v}_1+(\frac{1}{\tau_{c\rho}}+\frac{1}{\tau_K})(\frac{p_1}{p_0})+(\frac{1}{\tau_{cT}}-\frac{1}{\tau_{c\rho}}-\frac{1}{\tau_K})(\frac{\rho_1}{\rho_0})=0 \tag{22}$$

$$\frac{d\mathbf{B}_1}{dt}+i\mathbf{B}_0(\tilde{\boldsymbol{k}}\cdot\boldsymbol{v}_1)-i(\tilde{\boldsymbol{k}}\cdot\mathbf{B}_0)\boldsymbol{v}_1+\frac{2da/dt}{a}\mathbf{B}_1+\tilde{\boldsymbol{k}}\times\{\frac{\mathbf{B}_0}{4\pi\eta\epsilon\rho_0^{1+\nu}}\times[\mathbf{B}_0\times(\tilde{\boldsymbol{k}}\times\mathbf{B}_1)]\}=0 \tag{23}$$

where $c_s=\sqrt{\gamma p_0/\rho_0}$ and $\tilde{\boldsymbol{k}}=\boldsymbol{k}/a$ are, respectively, the adiabatic background sound speed and the Eulerian wave vector. The other symbols have the following definitions:

$$\tau_s\equiv\frac{1}{\tilde{k}c_s},\quad \tau_g\equiv\frac{1}{\sqrt{4\pi G\rho_0}},\quad \tau_K\equiv\frac{R\rho_0}{\mu(\gamma-1)K\tilde{k}^2}, \tag{24}$$

$$\tau_{cT}\equiv\frac{RT_0}{\mu(\gamma-1)\rho_0(\partial\Omega/\partial\rho)_T},\quad \tau_{c\rho}\equiv\frac{R}{\mu(\gamma-1)(\partial\Omega/\partial T)_\rho}; \tag{25}$$

that are the characteristic time-scale of sound waves, self-gravity perturbation waves, thermal conduction, isothermal differential cooling, and isobaric differential cooling, respectively.

We use the coordinate system $\boldsymbol{u}_x,\boldsymbol{u}_y,\boldsymbol{u}_z$ as specified by NG. Equations (21) and (23) may be used to uncouple v_{1y}- the perturbed velocity in the plane perpendicular to both $\mathbf{B}_0$ and $\boldsymbol{k}$- from the rest of the problem. With the choice of exponential perturbation (e^{ht}), disturbances perpendicular to the ($\mathbf{B}_0-\boldsymbol{k}$)-plane, have a solution which displays existence or non-existence of the Alfvén waves. Amplitude of the Alfvén waves are damped via expansion of the medium and/or with ion-neutral friction, while, it must grow with injection of energy in contracting medium.

The motion in the other modes are constrained to the $x-z$-plane, and are governed by the matrix equation,

$$Y^{(1)}=AY \tag{26}$$

where Y is a 5×1 matrix as follows:

$$Y=\begin{pmatrix}\rho_1/\rho_0\\ p_1/p_0\\ av_{1x}\\ av_{1z}\\ \sin\theta(\frac{B_{1z}}{B_0})-\cos\theta(\frac{B_{1x}}{B_0})\end{pmatrix},$$

and $Y^{(1)}$ is its first time derivative. The 5×5 matrix of the coefficients, A, is defined as

$$A = \begin{pmatrix} 0 & 0 & -\frac{i\sin\theta}{c_s\tau_s a} & -\frac{i\cos\theta}{c_s\tau_s a} & 0 \\ \frac{1}{\tau_{c\rho}} + \frac{1}{\tau_K} - \frac{1}{\tau_{cT}} & -\frac{1}{\tau_{c\rho}} - \frac{1}{\tau_K} & -\frac{i\gamma\sin\theta}{c_s\tau_s a} & -\frac{i\gamma\cos\theta}{c_s\tau_s a} & 0 \\ \frac{ic_s\tau_s a\sin\theta}{\tau_g^2} & \frac{ic_s a\sin\theta}{\gamma\tau_s} & 0 & 0 & -\frac{ic_s\tau_s a}{\tau_{AL}^2} \\ \frac{ic_s\tau_s a\cos\theta}{\tau_g^2} & \frac{ic_s a\cos\theta}{\gamma\tau_s} & 0 & 0 & 0 \\ 0 & 0 & -\frac{i}{c_s\tau_s a} & 0 & -\frac{1}{\kappa^2\tau_{AD}} \end{pmatrix},$$

where θ is the angle between $\boldsymbol{k}$ and $\mathbf{B}_0$, and

$$\tau_{AL} \equiv \frac{1}{\tilde{k}v_A} = \frac{\sqrt{4\pi\rho_0}}{\tilde{k}B_0}, \quad \tau_{AD} \equiv \frac{1}{\tilde{k}v_d} = \frac{4\pi\eta\epsilon\rho_0^{1+\nu}}{\tilde{k}^2(\kappa B_0)^2} \tag{27}$$

are the characteristic time-scales of the Alfvén waves and ambipolar diffusion, respectively.

3. Numerical Solutions

In this section we consider exponential growth rate and its characteristic equation (§3.1), the relative importance of the corresponding time-scales (§3.2), and some typical numerical data in the molecular clouds which lead to form oblate, prolate, and spherical condensations (§3.3).

3.1 Exponential Growth Rate

The standard exponential growth rate provides the following formal solution for all the perturbations:

$$y_{i(t)} = y_{i(t=0)} exp(ht), \tag{28}$$

where $real(h)$ represents their growth/decay rate. According to the background evolution, equations (15) and (16), we have

$$Y^{(1)} = hY + CY \tag{29}$$

where C is a diagonal matrix as

$$C \equiv \frac{1}{\tau_e} diag[3, 3\gamma, 1, 1, 2]. \tag{30}$$

where $\mid \tau_e \mid = \frac{a}{|da/dt|}$ represent contraction/expansion time-scale. Existence of solution for equation (26), needs the following condition:

$$Det[hI + C - A] = 0 \tag{31}$$

where I is the unitary matrix. According to this condition, we find a five-degree linear characteristic equation that without self-gravity and expansion/contraction of the background ($\tau_g, \tau_e \to \infty$), reduces to equation (22) of NG. We use the Laguerre method to find the roots of this characteristic equation.

3.2 Characteristic Time-Scales

A fundamental time-scale is the period of a sound wave, $\tau_s = 1/\tilde{k}c_s$, which can be rewritten as

$$\tau_s = 1.14 \times 10^7 \frac{\lambda_{(pc)}}{\sqrt{T_0}} a^2_{(\tau)} \quad year \tag{32}$$

where $\lambda_{(pc)}$ is the wavelength of perturbation in parsec. In the above equation and the subsequent equations, we choose the value of the polytropic index of the ideal gas as $\gamma = 5/3$. Other important time-scales are as follows:

3.2.1 *Self-gravity and Background Evolution*

(a)The characteristic time of background evolution is

$$\tau_e = \frac{a}{|da/dt|} = \frac{3.35 \times 10^7}{\sqrt{n_0}} \frac{a^{5/2}}{\dot{a}_{(\tau)}} \quad year \tag{33}$$

where n_0 is in the unit of cm^{-3}. This time is also the time-scale for the adiabatic temperature decrease/increase which follows from the expansion/contraction.
(b)The characteristic growth time of a perturbation by self-gravity is

$$\tau_g = \frac{1.9 \times 10^7}{\sqrt{n_0}} a^{3/2} \quad year \tag{34}$$

which coincides with the time-scale of the background deceleration (see equ.[17]).

3.2.2 *Thermal Conduction and Cooling*

(a)Thermal conduction coefficient of a molecular cloud, K, is given by (Lang 1986)

$$K \approx 2.16 \times 10^3 \sqrt{T_0}\, erg.s^{-1}.^oK^{-1}.cm^{-1}. \tag{35}$$

The characteristic time-scale of thermal conduction can be rewritten as

$$\tau_K = 2.80 \times 10^{10} \frac{n_0 \lambda^2_{(pc)}}{\sqrt{T_0}} \quad year. \tag{36}$$

(b)Inserting the net cooling function into definitions of the differential cooling time-scales; we obtain

$$\mid \tau_{cT} \mid = \frac{1.98 T_0}{\Lambda(n_0, T_0) a^2 \mid \delta + 2.5(\xi - 0.6\chi) \mid} \quad year \tag{37}$$

$$|\tau_{c\rho}| = \frac{1.98 T_0}{\Lambda(n_0, T_0) a^2 \mid \beta \mid} \quad year. \tag{38}$$

where ξ and χ are defined as

$$\xi \equiv \frac{\Gamma_{AD}}{\Lambda(n_0, T_0)}, \quad \chi \equiv \frac{\Gamma_{grav}}{\Lambda(n_0, T_0)}. \tag{39}$$

3.2.3 *Magnetic Field*

(a)The Characteristic time of the Alfvén wave is

$$\tau_{AL} = 6.20 \times 10^5 \sqrt{n_0} \frac{\lambda_{(pc)}}{B_{0(\mu G)}} a^{3/2} \quad year \tag{40}$$

where $B_{0(\mu G)}$ is the background magnetic field in the unit of microgauss.
(b)Time-scale of the ambipolar diffusion is

$$\tau_{AD} = 9.85 \times 10^4 n_0^{3/2} [\frac{\lambda_{(pc)}}{\kappa B_{0(\mu G)}}]^2 a^{3/2} \quad year \tag{41}$$

that displays the drift time (in the wavelength of perturbation) of the frozen ions relative to the neutrals.

The different characteristic times have different dependence on $\lambda_{(pc)}$, so the corresponding processes will be important in different wavelength domains. For instance, the conduction growth-rate and ambipolar diffusion time-scale, depend on wavelength as $\lambda^2_{(pc)}$. Hence, conduction and ambipolar diffusion dominate at short wavelengths. The differential cooling, background expansion and self-gravity time-scales have no spatial dependence. Hence, these processes are dominant at long wavelengths. The frequency of sound and Alfvén waves, finally, depends on the first power of $\lambda_{(pc)}$. Hence sound and Alfvén propagation could be the dominant effect at intermediate wavelengths. The boundaries between the different regions can be easily estimated using the definitions of the characteristic times just given.

3.3 Typical data for the molecular clouds

We present some typical data which correspond to the real observed magnetic molecular clouds. We consider the magnetic molecular clouds with density between $10^2 cm^{-3}$ to $10^5 cm^{-3}$, temperatures in the range of $T_0 \approx 10-100K$, and magnetic field strength $B_0 \approx 10\mu G$ (Myers & Goodman 1988, Crutcher 1999). It would be interesting to investigate

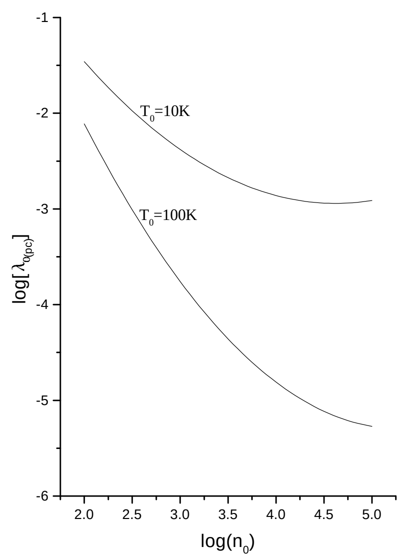

Figure 2. The Field length in the molecular clouds versus number density, $n_0(cm^{-3})$.

the perturbations with wavelengths around Field length (equation [26] of NG)

$$\lambda_{0(pc)} \equiv 8.4 \times 10^{-6} \frac{T_0^{3/4}}{n_0^{1/2} a \sqrt{\Lambda(n_0, T_0)\beta}}. \tag{42}$$

The values of the $\lambda_{0(pc)}$ for typical data in the molecular clouds is given in Fig. 2. According to this figure, we choose wavelengths in the range of $\lambda_{(pc)} \approx 10^{-4} - 10^{-1} pc$, that are interesting in formation of the small-scale condensations.

Firstly, we consider the sound domain where time-scale of the sound wave is much smaller than other time-scales. The characteristic equation reduces to a three-degree linear equation that has three solutions: two sound waves and one condensation mode. Stable and unstable regions in the $log(n_0) - log[\lambda_{(pc)}]$ plane, for typical values of $\xi - 0.6\chi$ equal to 1.0 and -1.0, are shown in Fig. 3.

We now study the effect of the self-gravity and the expansion/contraction of background. If the background is expanding, its expansion energy causes the medium to stabilize in the isentropic instability case. On the other hand, in the isobaric instability case, ion-neutral friction increases pressure, thus, it only causes stabilization of the medium in the direction perpendicular to the magnetic field. Therefore, the oblate condensations

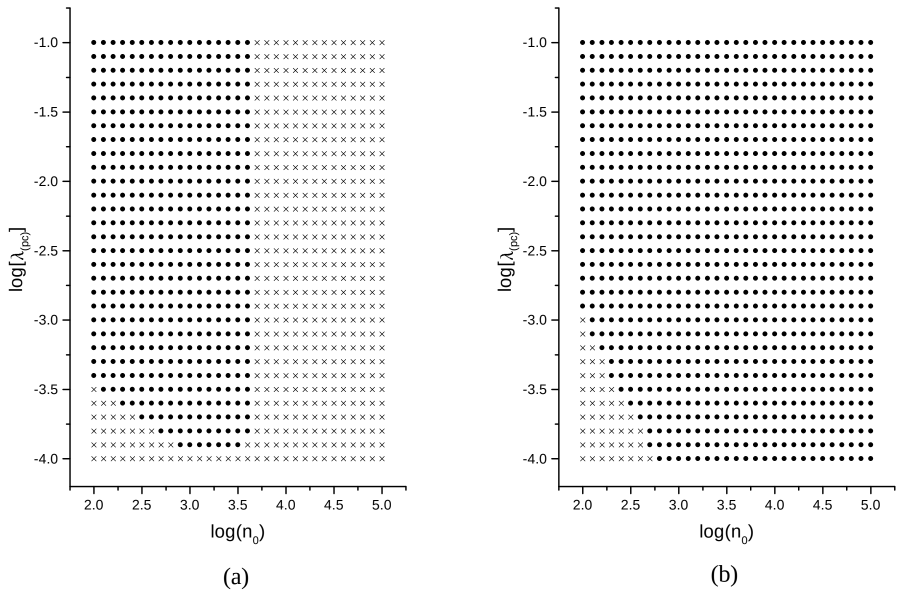

Figure 3. The stable($\times$) and unstable($\bullet$) regions for typical values of (a)$\xi - 0.6\chi = 1.0$ with temperature $T_0 = 10K$, and (b)$\xi - 0.6\chi = -1.0$ with temperature $T_0 = 100K$, in the sound domain of the molecular clouds.

can be produced. This case is shown in Fig. 4, for a typical value of $\xi - 0.6\chi = 1.0$ and $\dot{a}_{(\tau=0)} = 0.5$.

For a contracting background, contraction energy is injected into the medium. Thus, its stability is decreased and converted to a prolate instability. Diffusion of neutrals relative to the frozen ions in the perpendicular direction of the magnetic field is the reason of this prolate instability. This case is shown in Fig. 5 for typical values of $\xi - 0.6\chi$ equal to 1.0 and -1.0, with temperature $T_0 = 10$ and $100K$. Whenever the local parameters of a magnetic molecular cloud, lie within this $log(n_0) - log[\lambda_{(pc)}]$ plane, prolate condensation may be produced via thermal instability.

4. Summary and prospects

In this paper we perform linear analysis of thermal instability in locally uniform expanding/contracting magnetic molecular clouds which, in the perturbed state, is undergoing ambipolar diffusion. Thermal conduction and self-gravity have also been included as fundamental ingredients. The small-perturbation problem yields a system of ordinary

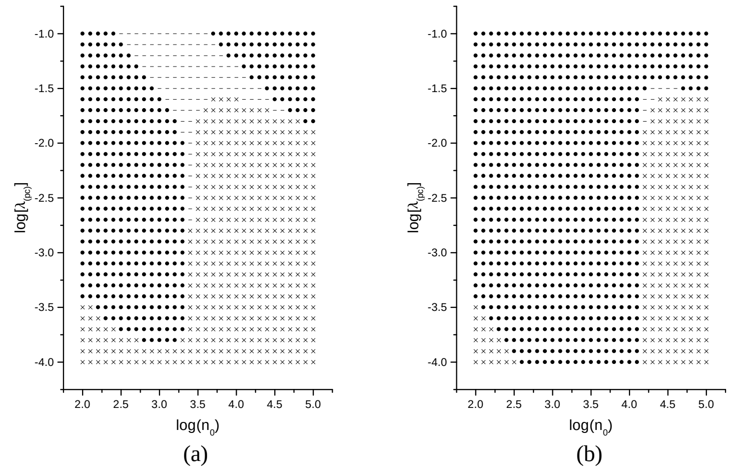

Figure 4. The stable($\times$), spherical instability($\bullet$), and oblate instability($-$) for typical value of $\xi - 0.6\chi =$ $= 100K$.

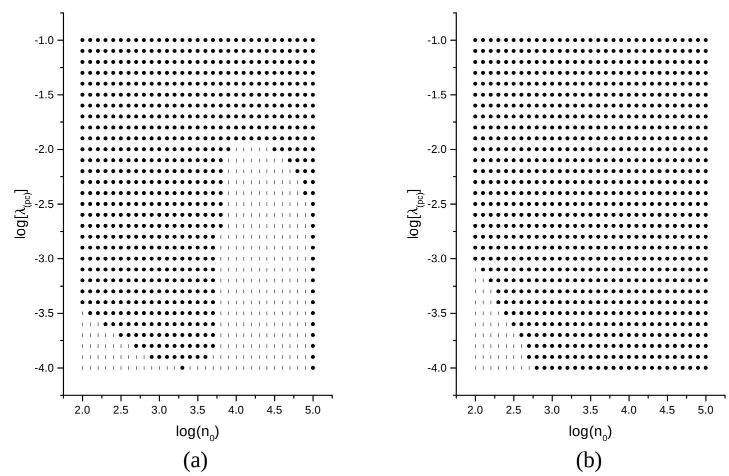

Figure 5. The spherical instability($\bullet$) and prolate instability($|$) in contracting background with $\dot{a}_{(\tau=0)} = -0.1$, for typical values of a)$\xi - 0.6\chi = 1.0$ with temperature $T_0 = 10K$, and (b)$\xi - 0.6\chi = -1.0$ with temperature $T_0 = 100K$.

differential equations with five independent solutions. We choose an exponential growth rate, which converts the system of ordinary differential equations into a five-degree complete characteristic equation. If we neglect the self-gravity and expansion/contraction of the background, the characteristic equation reduces to the prior results of NG. We have used the Laguerre method to find the roots of this complete characteristic equation.

In sound domain, two of the solutions have the character of oscillatory modes (sound waves) and the third one is a non-oscillatory (or condensation) solution. We adopt a parametric net cooling function and find for perturbations with wavelengths greater than the Field lengths, thermal instability causes the medium to condense. Fig. 3 shows different stable and unstable regions in the molecular clouds and their cooling rates are presented in Fig. 1.

We choose a wide range of density and temperature in the molecular clouds with typical magnetic field strength $B_0 \approx 10\mu G$. Interesting wavelengths in the problem are around the Field length which is shown in Fig. 2. According to this figure, we consider wavelengths around $10^{-4}-10^{-1}pc$ for small-scale condensations. Different stable and unstable regions of the $log(n_0) - log[\lambda_{(pc)}]$ plane for the sound domain are shown in Fig. 4 and Fig. 5 for expanding and contracting backgrounds, respectively. In the expanding background, expansion energy in the isentropic instability, causes to stabilizes the medium in the direction of the magnetic field and perpendicular to it, while, in the isobaric instability it only stabilizes the medium in the perpendicular direction. In the contracting background, stability of the medium is decreased and converted to the prolate instability via injection of contraction energy.

In this paper we conclude that linear thermal instability can produce small-scale condensations in spherical, oblate, or prolate shapes. We try to analyze, linearly, a rather involved problem, because, before nonlinear regime overcomes, *turbulence* causes interaction and merging of these incompletely formed condensations. Physically, we expect that merging of these small-scale condensations culminate in the large-scale clumps that are star bearing regions in our world. We are now preparing a complete simulated turbulent magnetic molecular cloud with condensations produced by thermal instability. We will investigate the effect of interaction and merging of these small-scale condensations with smoothed particle hydrodynamics (SPH) method.

References

Arons J., Max C. E., 1975, *Astrophys. J.*, **196**, L77.
Basu S., 2000, *Astrophys. J.*, **540**, L103.
Crutcher R. M., 1999, *Astrophys. J.*, **520**, 706.
Draine B. T., 1986, *Mon. Not. R. Astron. Soc.*, **220**, 133.
Falgarone E., Puget J. L., Pérault C. K., 1992, *Astron. Astrophys.*, **257**, 715.
Fiege J. D., Pudritz R. E., 2000, *Astrophys. J.*, **534**, 291.
Gammie C. F., Lin Y., Stone J. M., Ostriker E. C., 2003, *Astrophys. J.*, **592**, 203.
Gilden D. L., 1984, *Astrophys. J.*, **283**, 679.
Glassgold A. E., Langer W. D., 1974, *Astrophys. J.*, **193**, 73.
Goldsmith P. F., Langer W. D., 1978, *Astrophys. J.*, **222**, 881.
Hartmann L., 2002, *Astrophys. J.*, **578**, 914.
Hennebelle P., 2003, *Astron. Astrophys.*, **397**, 381.
Indebetouw R., Zweibel E. G., 2000, *Astrophys. J.*, **532**, 361.
Jones C. E., Basu S., 2002, *Astrophys. J.*, **569**, 280.

Lang K. R., 1986, *Astrophysical Formula*, 2nd edn, Springer-Verlag, Berlin, p. 320.
Larson R. B., 1981, *Mon. Not. R. Astron. Soc.*, **194**, 809.
Liszt H., Lucas, R., 2000, *Astron. Astrophys.*, **355**, 333.
McDaniel E. W., Mason E. A., 1973, *The Mobility And Diffusion of Ions in Gases*, New York: Wiley, p. 127.
Moore E. M., Marscher A. P., 1995, *Astrophys. J.*, **452**, 679.
Myers P. C., Goodman A. A., 1988, *Astrophys. J.*, **329**, 392.
Nejad-Asghar M., Ghanbari J., 2003, *Mon. Not. R. Astron. Soc.*, **345**, 1323.(NG)
Nelson R. P., Langer W. D., 1997, *Astrophys. J.*, **482**, 796.
Neufeld D. A., Leep S., Melnick G. J., 1995, *Astrophys. J. Supp.*, **100**, 132.
Pan K., Federman S. R., Welty D. E., 2001, *Astrophys. J.*, **558**, L105.
Peng R., Langer W. D., Velusamy T., Kuiper T. B. H., Levin S., 1998, *Astrophys. J.*, **497**, 842.
Rollinde E., Boissé P., Federman S. R., Pan K., 2003, *Astron. Astrophys.*, **401**, 215.
Ryden B. S., 1996, *Astrophys. J.*, **471**, 822.
Sakamoto S., Sunada K., 2003, *Astrophys. J.*, **594**, 340.
Shu F., 1992, *The Physics of Astrophysics*, Vol II., University Science Books, Mill Valley, CA, p. 360.
Solomon P. M., Rivolo A. R., Barrett J., Yahil A., 1987, *Astrophys. J.*, **319**, 730.
Umebayashi T., Nakano T., 1980, *Pub. Astron. Soc. Japan*, **32**, 405.